Electronic Supplementary Material (ESI) for Chemical Communications.

Supporting Information

Measuring and Modelling Mechanochemical Reaction Kinetics

Alejandro Boscoboinik, Dustin Olson, Heather Adams,‡ Nicholas Hopper and Wilfred T. Tysoe

Department of Chemistry and Biochemistry and laboratory for Surface Studies, University of Wisconsin-Milwaukee, Milwaukee, WI 53211, USA

‡ *Present address: Alcami Corporation, Germantown, WI 53022, USA*

Table of Contents

Materials and Methods

Experiments were carried out using an RHK Variable Temperature Ultrahigh Vacuum (UHV) 750 atomic force microscope (AFM) operating at a base pressure of ~2×10^{-10} Torr following bakeout. The apparatus also contained an analysis chamber for sample cleaning and was equipped with a Scienta Omicron SPECTALEED combined low-energy electron diffraction (LEED)/Auger system for assessing sample cleanliness and crystalline order. The chamber was also equipped with a Dycor quadrupole mass analyzer for leak checking and background gas analysis. The Cu(100) single crystal was cleaned by Argon ion bombardment (~1 kV, ~2 $\mu A/cm^2$) and then by annealing to ~850 K to remove any surface damage induced by the cleaning procedure. A saturated overlayer of methyl thiolate species was prepared by dosing a clean Cu(100) sample held at ~298 K in UHV by background dosing at a pressure of 1×10^{-8} Torr of dimethyl disulphide (DMDS, Aldrich, 99.0% purity) for 200 s, where the pressure was measured using a nude ionization gauge included in the UHV chamber, where the pressures were not corrected for ionization gauge sensitivity.[1] The DMDS was transferred to a glass bottle and attached to the gas-handling system of the vacuum chamber and cleaned by several freeze-pump-the cycles. The purity was monitored using mass spectroscopy. Sulphur overlayers were prepared by decomposing a methyl thiolate overlayer on Cu(100) by heating to ~430 K for 300 s.

Normal-stress-induced mechanochemical reaction kinetics were measured by applying a normal force using a silicon μ-masch (HQ:NSC19/NO AL) AFM tip with a nominal 8 nm radius. The cantilever force constant was obtained from the geometry of the cantilever measured by scanning electron microscopy (SEM, Figures S1(a) and (b)) as described in reference.[2] SEM was also used to verify the integrity of the AFM tip prior to performing the experiments (Figures S2(c) and (d)). Because the pressure varies as a function of distance from the centre of the contact for elastic contact of a spherical tip on a planar substrate,[3] the extent of reaction under normal load as a function of time was measured from the depth at the centre of the indent formed on the methyl-thiolate-saturated surface measured using contact AFM using a non-perturbative load using a scan area of 0.1 μm× 0.1 μm over the pre-indented region. Force-distance curves (Figure S3) measured between each indentation experiment verified that the tip shape had not changed. The tips were found to remain stable over multiple indentation experiments. However, to verify that the nature of the tip did not influence the results, normal-stress-induced reaction rates were measured with two different tips.

Density functional theory (DFT) calculations of methyl thiolate species adsorbed on Cu(100) were performed with the projector augmented wave method [4, 5] as implemented in the Vienna *ab initio* simulation package, VASP.[6-8] The exchange-correlation potential was described using the generalized gradient approximation of Perdew, Burke and Ernzerhof.[9] A cut-off of 400 eV was used for the planewave basis set, and the wavefunctions and electron density were converged to within 1×10^{-6} eV. The first Brillouin zone was sampled with a 7×7×1 Monkhorst-Pack grid.[10] Geometric relaxations were considered to be converged when the force was less than 0.01 eV/Å on all unrestricted atoms.

Compression of the cell and climbing nudged elastic band (cNEB) calculations were performed as a function of normal stress on a 3×3×6 Cu(100) slab with the top three layers left free to relax and the bottom three layers frozen to mimic the influence of the bulk crystal. A 3×3×3 slab of Cu atoms with fixed positions was added above the

bottom slab with a vacuum layer above the upper slab, shown in Figure S4. The k-point mesh and vacuum layer were varied to find a reproducible energy. For these calculations, the first Brillouin zone was sampled with a 4×4×1 Monkhorst-Pack grid. The upper slab was lowered in increments of 0.2 Å and the system was allowed to relax before moving the slab another step. Incremental lowering was necessary to ensure reproducible results for each value of compression.

In all cases, activation energies were calculated using the climbing image nudged elastic band (cNEB) method. The initial and final states were first calculated with DFT and a linear interpolation of the atomic positions was used to determine the initial positions of the starting nudged elastic band (NEB) images.[11, 12]

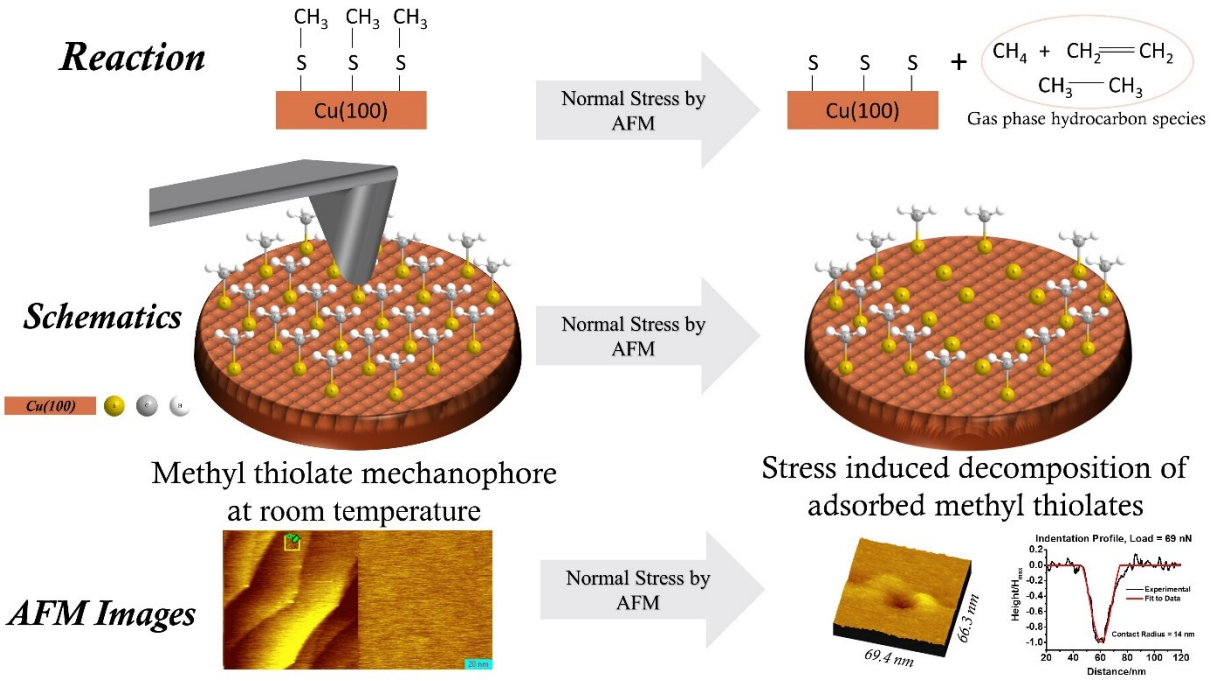

Figure S1. Schematic depiction of the mechanochemical experiment and the reaction pathway.

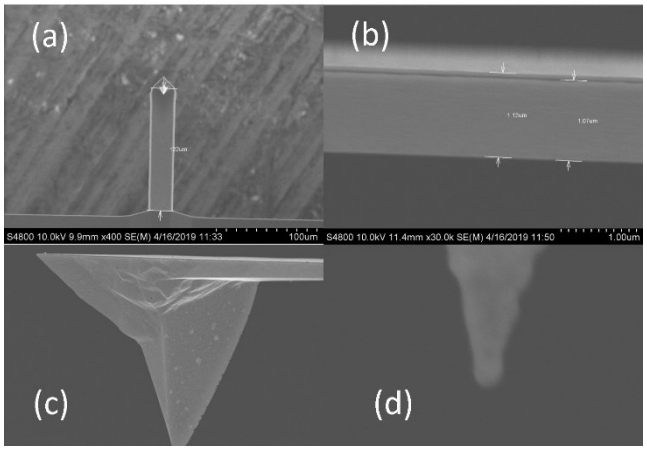

Figure S2. Scanning electron microscopy images of the AFM tips. (a) top view of the cantilever, (b) side view of the cantilever, (c) low-magnification view of the silicon tip prior to the experiment and (d) high-magnification image of the tip prior to the experiment.

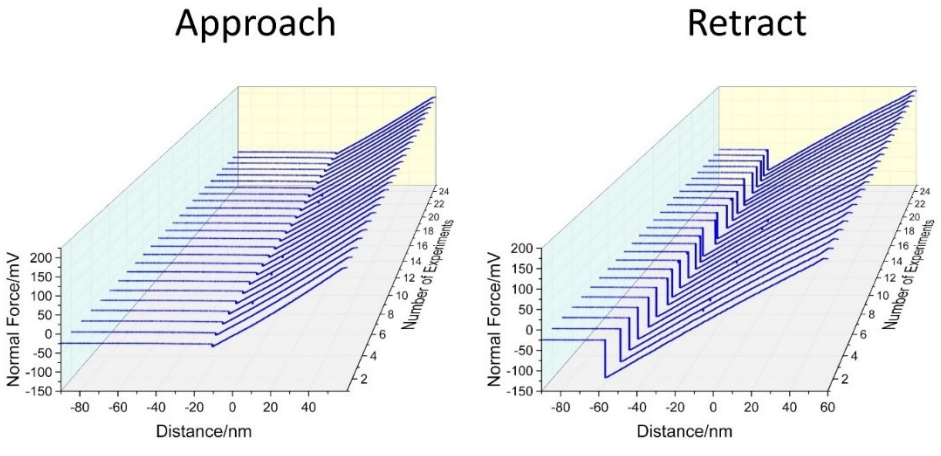

Figure S3. A series of sequential force-distance curves for a saturated methyl thiolate overlayer adsorbed on Cu(100) at 298 K by exposure to DMDS

showing the Approach and Retract curves.

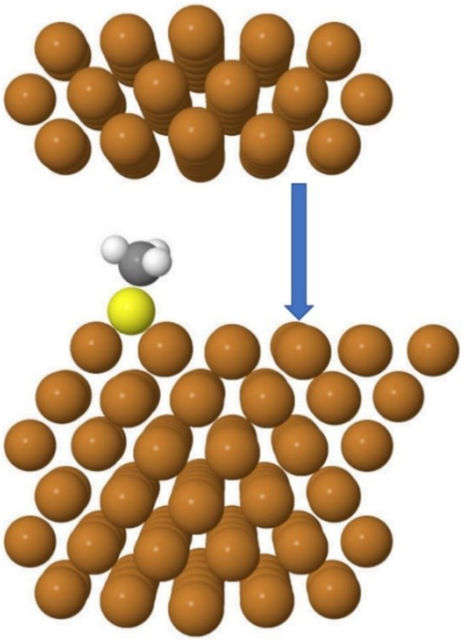

Figure S4. Depiction of the configuration used for the DFT calculations of a methyl thiolate overlayer on Cu (100) with a top slab of Cu (100) at an initial distance of 8 Å from the bottom, lowered in 0.2 Å steps.

Indentation Profiles, Reaction Rates and Pressure Distribution

The depth of the indent is proposed to be directly proportional to the extent of the reaction. This assumption is tested by comparing the experimental indentation profile with that calculated using this assumption. The normal stress distribution $\sigma(r)$ for an elastic contact of a sphere against a flat surface is given by $\sigma(r) = \sigma_0\sqrt{\left(1-\frac{r^2}{a^2}\right)}$, where σ_0 is the normal contact stress at the center of the contact and a is contact radius.[3] According to the Bell model, the rate depends exponentially on the stress: $k(\sigma) = k_0 exp\left(\frac{\sigma\Delta V^{\ddagger}}{k_B T}\right)$, where $\Delta V^{\ddagger}$ is the activation volume, which is measured to be ~46 Å^3. This will result in mechanochemical reactions occurring more rapidly at the centre of the contact, with the rate decreasing to zero at the edges; the maximum radius of the normal-stress induced indentation provides a direct measure of the contact radius.[13] Thus, the indentation profile should reflect both the stress distribution and the rate at which the methyl thiolate decomposes mechanochemically. If the depth is proportional to the extent of reaction, this yields a depth profile $d(r)$ given by $d(r) \propto exp\left(\frac{\sigma(r)\Delta V^{\ddagger}}{k_B T}\right)$. To test whether the postulate is valid, experimental depth profiles were compared to this equation by normalizing the depth to unity and by using $\Delta V^{\ddagger}$ = 46 Å^3. A typical result is shown in Fig. S5, in this case, for an experiment using a load of 69 nN. The agreement between experiment and theory is in accord with the postulate that the indentation profiles are mechanochemically induced, and that the indentation depth at the centre of the profile is a measure of the mechanochemical reaction rate. In this case, the normal stress at the centre of the contact is given by $\sigma_0 = \frac{1.5F_N}{\pi a^2}$ where $F_N$is the normal force exerted by the AFM tip.

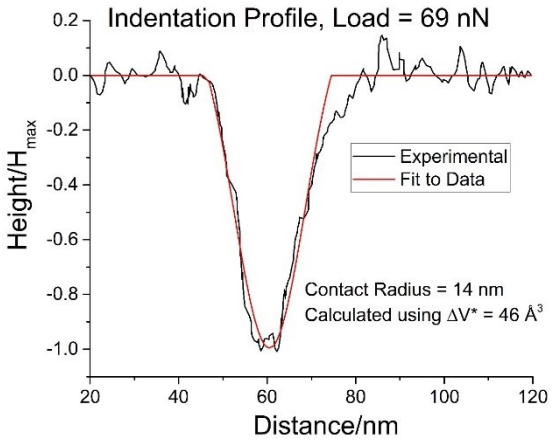

Figure S5. Typical indentation profile formed by compressing a methyl-thiolate saturated Cu(100) surface at a load of 69 nN for 9×10^3 s, compared to a fit for an elastic contact using an activation volume of 46 Å^3 by assuming that the indentation depth is proportional to the extent of reaction.

Measurement of Reaction Rates and Activation Energies

Previous experiments to measure the rate of stress-activated decomposition of methyl thiolate species on copper from the evolution of gas-phase products [14] show that the reaction is first order in methyl thiolate coverage: $-\frac{d\theta_{th}}{dt} = k(\sigma)\theta_{th}$, where θ_{th} is the relative coverage of methyl thiolate species. Taking the initial relative methyl thiolate coverage to be unity and integrating the rate equation gives: $\theta_{th}(t) = (1 - exp(-k(\sigma)t))$, and fits to this equation, carried out using Origin software, are shown in Figs. 1 and S6, confirming that methyl thiolate decomposition on Cu(100) measured by AFM under the influence of a normal stress obeys first-order kinetics over the whole coverage range. Note that attempts to fit that data to other reaction orders yielded much worse fits that the first-order kinetics shown in Figs 1 and S6. The values of k_0 and $\Delta V^{\ddagger}$ are extracted directly from plots of

$ln(k(\sigma_0))$ versus σ_0 (Fig. 2) where the intercept equals $ln(k_0)$ and the slope is $\Delta V^{\ddagger}/k_B T$, where T is the reaction temperature (298 K). An activation energy is obtained from k_0 by assuming an pre-exponential factor of 1×10^{14} s^{-1}.[15]

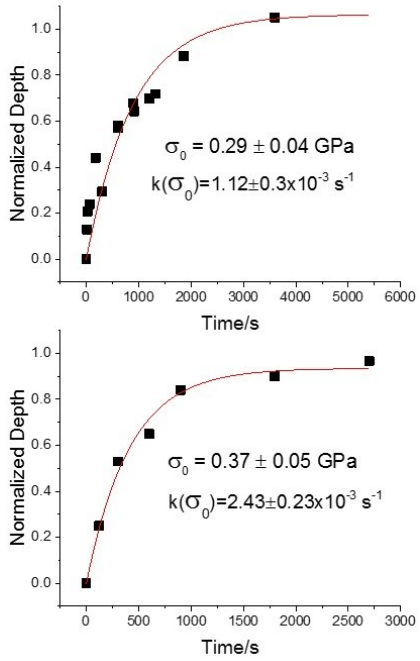

Figure S6. Typical plots of normalized indention depth as a function of time showing fits to first order mechanochemical reaction rates for maximum contact pressures of 0.29 and 0.37 GPa.

Control Experiments

In order to ensure that the indentation was not due to plastic deformation of the Cu(100) substrate, a sulphur overlayer was formed on Cu(100) to prevent adhesion between the tip and the substrate by heating a methyl thiolate overlayer to 430 K for 300 s. A low-load image showed a flat surface (Figure S7(a)). The center of the scanned region (indicated by a red dot in Figure S7(b)) was then compressed using a load of ~92 nN for 1.2×10^4 s and showed no indentation when imaged with a load of ~25 nN (Figure S7(c)). This confirms that the indents formed on methyl-thiolate covered copper are due to methyl thiolate decomposition.

To establish whether the imaged profiles of the indented regions were not perturbed by scanning at low loads, the evolution of the images of the indented surface was monitored by repeatedly collecting images of a methyl-thiolate-covered Cu(100) surface that had been indented at a load of ~52 nN for 9×10^3 s; this removes ~50% of the methyl thiolate layer. The evolution of the surface as a function of the number of passes of the AFM tip over the indented surface at a low load is shown in Movie S2. Profiles across the indent were analysed as a function of the number of scans of the AFM tip by fitting the profile to a Gaussian function. This shows that the area under the profile shows no significant variation as a function of the number of scans (Figure S8(a)). However, the width of the indented regions does vary as a function of the number of scans (Figure 8(b)), where a sigmoidal function is shown plotted with the data as a guide to the eye. This reveals that the width of the indented area depends on the number of times the indent was scanned. However, no variation in the width of the indent was found for the first three scans.

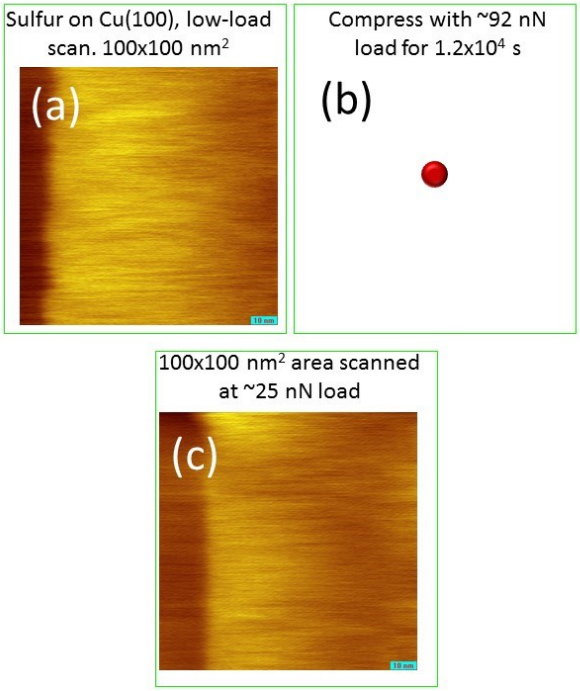

Figure S7. Image of a 100 nm × 100 nm area of a sulphur-covered Cu(100) surface collected at a low load (a), and then compressed at the centre point indicated by a red dot using a load of ~92 nN for 1.2×10^4 s (b). The same region was then imaged at a load of ~25 nN (c) and showed no indentation.

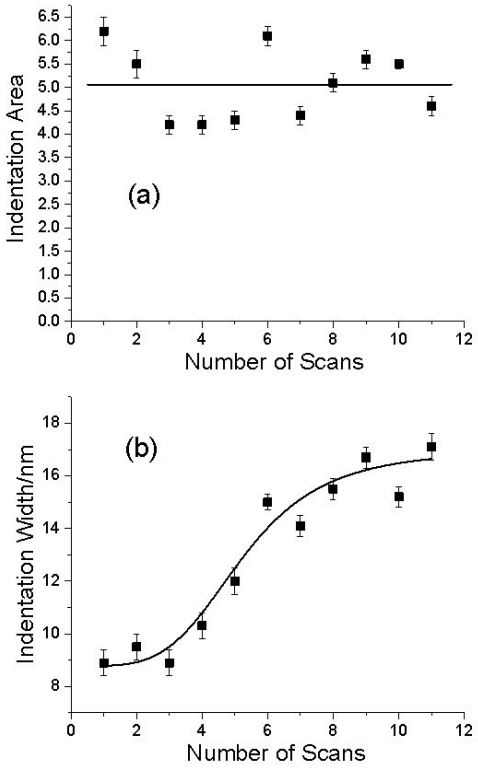

Figure S8. Plot of the evolution of a methyl thiolate overlayer on Cu (111) indented at ~52 nN for 9×10^3 s to remove ~50% of the methyl thiolate layer as a function of the number of scans when scanning at low load, where the variation in the images is shown in Movie S2, displaying (a) the variation in the indented area and (b) the variation in the indented width as a function of the number of scans.

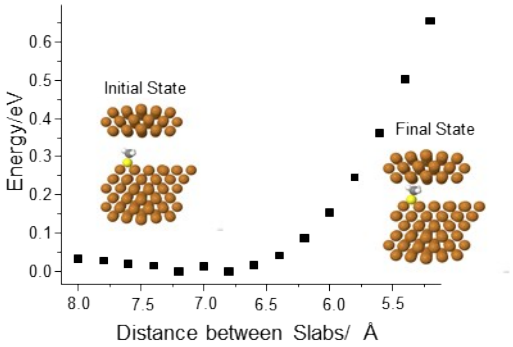

Figure S9: DFT calculations were carried out for CH_3–$C_{(ads)}$ on a Cu(100) slab as a function of slab separation, where the normal stress was calculated from the change in energy as a function of distance from the repulsive part of the potential.

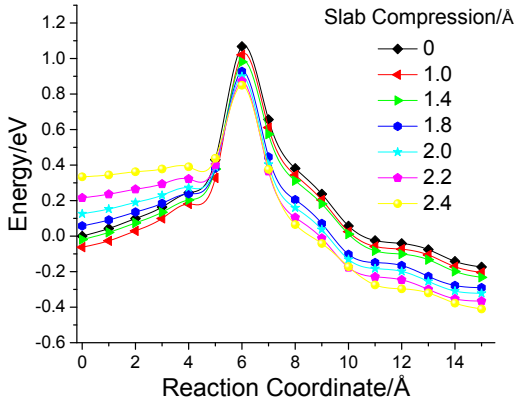

Figure S10. Energy profiles yielded by nudged elastic band (NEB) calculations.

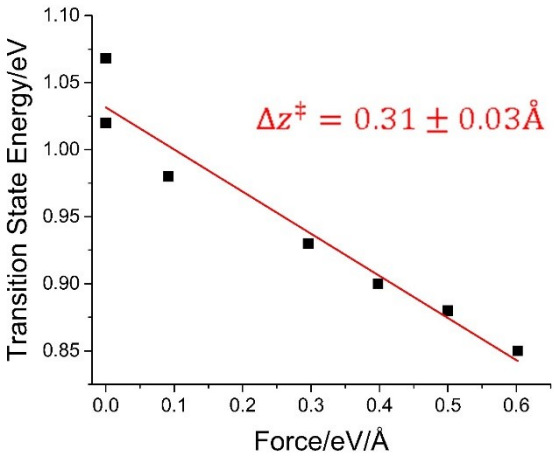

Figure S11. Plot of the energy of the transition state for DFT calculations of methyl thiolate on Cu(100) versus normal force, leading to a calculated value of $\Delta z^{\ddagger}$ of 0.31 ± 0.03 Å.

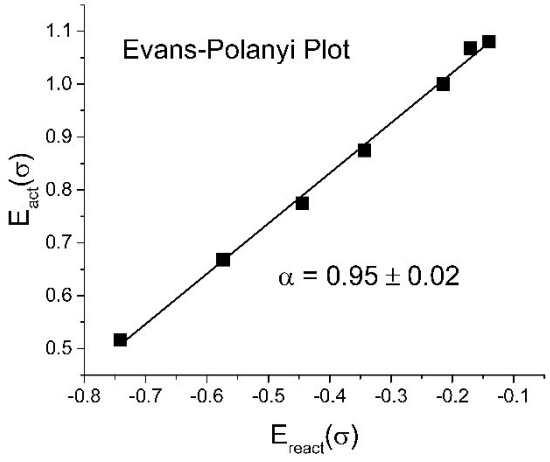

Figure S12. Evans-Polanyi plot of the activation energy for methyl thiolate decomposition on Cu(100) as a function of the normal stress, $E_{act}(\sigma)$ versus energy of reaction as a function of the normal stress, $E_{react}(\sigma)$ leading to a value of the slope, α of 0.95 ± 0.02.

References

1. O. J. Furlong, B. P. Miller, Z. Li, J. Walker, L. Burkholder and W. T. Tysoe, *Langmuir*, 2010, **26**, 16375-16380.
2. E. Meyer, H. J. Hug and R. Bennewitz, *Scanning probe microscopy : the lab on a tip*, Springer, Berlin; London, 2011.
3. K. L. Johnson, *Contact mechanics. Cambridge University Press: Cambridge [Cambridgeshire]; New York, 1985.*.
4. G. Kresse and D. Joubert, *Physical Review B*, 1999, **59**, 1758-1775.
5. P. E. Blöchl, *Physical Review B*, 1994, **50**, 17953-17979.
6. G. Kresse and J. Hafner, *Physical Review B*, 1993, **47**, 558-561.
7. G. Kresse and J. Furthmüller, *Physical Review B*, 1996, **54**, 11169-11186.
8. G. Kresse and J. Furthmüller, *Computational Materials Science*, 1996, **6**, 15-50.
9. J. P. Perdew, K. Burke and M. Ernzerhof, *Physical Review Letters*, 1996, **77**, 3865-3868.
10. H. J. Monkhorst and J. D. Pack, *Physical Review B*, 1976, **13**, 5188-5192.
11. G. Henkelman, B. P. Uberuaga and H. Jonsson, *The Journal of Chemical Physics*, 2000, **113**, 9901-9904.
12. G. Henkelman and H. Jónsson, *The Journal of Chemical Physics*, 2000, **113**, 9978-9985.
13. J. R. Felts, A. J. Oyer, S. C. Hernández, K. E. Whitener Jr, J. T. Robinson, S. G. Walton and P. E. Sheehan, *Nature Communications*, 2015, **6**.
14. H. Adams, B. P. Miller, O. J. Furlong, M. Fantauzzi, G. Navarra, A. Rossi, Y. Xu, P. V. Kotvis and W. T. Tysoe, *ACS Applied Materials & Interfaces*, 2017, **9**, 26531-26538.
15. H. L. Adams, M. T. Garvey, U. S. Ramasamy, Z. Ye, A. Martini and W. T. Tysoe, *The Journal of Physical Chemistry C*, 2015, **119**, 7115-7123.